STUDY AND ANALYSIS OF THREE PORT DC-DC CONVERTER IN DUAL INPUT MODE FOR STANDALONE PV SYSTEM

Thesis submitted in partial fulfillment of the requirements for the degree of

Master of Technology

in

Electrical Engineering
(Specialization: Control & Automation)

by

Pramisha Shukla

Department of Electrical Engineering
National Institute of Technology Rourkela
Rourkela, Odisha, 769008, India
May 2015

STUDY AND ANALYSIS OF THREE PORT DC-DC CONVERTER IN DUAL INPUT MODE FOR STANDALONE PV SYSTEM

Dissertation submitted in

in May 2015

to the department of

Electrical Engineering

of

National Institute of Technology Rourkela

in partial fulfillment of the requirements for the degree of

Master of Technology

by

Pramisha Shukla

(Roll 213EE3313)

under the supervision of

Prof. Susovon Samanta

Department of Electrical Engineering
National Institute of Technology Rourkela
Rourkela, Odisha, 769008, India

May 2015

Department of Electrical Engineering
National Institute of Technology Rourkela
Rourkela-769008, Odisha, India.

Certificate

This is to certify that the work in the thesis entitled "Study And Analysis Of Three Port DC-DC Converter In Dual Input Mode For Standalone PV Syatem" by Pramisha Shukla is a record of an original research work carried out by him under my supervision and guidance in partial fulfillment of the requirements for the award of the degree of Master of Technology with the specialization of Control & Automation in the department of Electrical Engineering, National Institute of Technology Rourkela. Neither this thesis nor any part of it has been submitted for any degree or academic award elsewhere.

Place: NIT Rourkela
Date: May, 2015

Prof. Susovon Samanta
Professor, EE Department
NIT Rourkela, Odisha

ACKNOWLEDGEMENT

First and Foremost, I would like to express my sincere gratitude towards my supervisor Prof. Susovon Samanta for his advice during my project work. He has constantly encouraged me to remain focused on achieving my goal. His observations and comments helped me to establish the overall direction of the research and to move forward with investigation in depth. He has helped me greatly and been a source of knowledge.

I extend my thanks to our HOD, Prof. A.K Panda and to all the professors of the department for their support and encouragement.

I am really thankful to my batch mates, especially Amit, Krishnaja, Rahul and Preeti who helped me during my course work and also in writing the thesis . Also I would like to thanks my seniors particularly Murli and Mahendra Sir for their support. My sincere thanks to everyone who has provided me with kind words, a welcome ear, new ideas, useful criticism, or their invaluable time, I am truly indebted.

I must acknowledge the academic resources that I have got from NIT Rourkela. I would like to thank administrative and technical staff members of the Department who have been kind enough to advise and help in their respective roles.

Last, but not the least, I would like to acknowledge the love, support and motivation I received from my parents and therefore I dedicate this thesis to my family.

PRAMISHA SHUKLA
213EE3313

LIST OF ABBREVIATION

BCR	: Battery Current Regulation
BVR	: Battery Voltage Regulation
CCM	: Continuous Conduction Mode
D	: Duty cycle
DI	: Dual Input
DO	: Dual Output
DIC	: Dual Input Converter
DOC	: Dual Output Converter
IVR	: Input Voltage Regulation
MIC	: Multiple Input Converter
MIMO	: Multiple Input Multiple Output
MPPT	: Maximum Power Point Tracking
MOSFET	: Metal Oxide Semiconductor Field Effect Transistor
OVR	: Output Voltage Regulation
PCSC	: Pulsating Current Source Cell
P&O	: Perturb And Observe
PV	: Photo-Voltaic
PVSC	: Pulsating Voltage Source Cell
PWM	: Pulse Width Modulation
SISO	: Single Input Single Output

TPC : Three Port Converter

VCCS : Voltage Controlled Current Source

ABSTRACT

This paper aims at designing and modelling of three port DC-DC converter and also describes the power management for multiple sources by using three port DC-DC converter based on boost topology. These multiple input converters are capable enough in independent and simultaneous regulation of either of two ports whereas the third port balances the power in entire system. The Multiple input converter (MIC) instead of conventional converters has several advantages such as high efficiency, reduced conversion stages, lower cost, more compact packing, excellent management of the power among the ports and provides centralized control. The three port converter (TPC) topology based on dual input converter (DIC) or dual output converter (DOC) interfaces one PV panel as input source port, one synchronous battery port, and an output/load port. As there are numerous modes of operations, so independent power management in each port is a challenging task. This TPC works in dual input mode (DI), dual output mode (DO), and single input single output mode (SISO). This paper explains detail analysis of all the three modes. Finally, in order to obtain design equations DI mode is analyzed in detail. State space averaging has been developed to obtain various transfer functions under DI mode. Pulse width modulation scheme for the Boost TPC has been designed in order to get smooth autonomous mode transition. A controller has been designed and simulated by using perturb and observe (P&O) MPPT method and output voltage regulation.

Table of Contents

Table of Figures

CHAPTER 1

INTRODUCTION

1.1 BACKGROUND

Solar power was first time captured by John Herschel in a collector box to cook food. They use solar power in two ways i.e. firstly heat can be trapped in the form of thermal energy and then converted into electrical energy by using photovoltaic (PV) cells. As the reserve of the fossil fuels are rapidly diminishing so now renewable energy resources are the alternative. Nowadays Renewable energy sources are in huge demand because they are inexhaustible, and their abundance availability in nature. In addition to this, due to combustion of fossil fuel create pollution. Unlikely, renewable energy sources are cleaner and produces energy without inducing pollution. Due to huge demand of electrical energy, production of electricity from solar energy using photovoltaics (PV) has catch the attention of researchers. Inspite having numerous merits, PV panel has some demerits also such as high cost, low efficiency and high power PV farm construction is required. Maximum power point tracking (MPPT) is used to enhance the efficiency of PV cell. PVs can be interfaced with wide range of loads and energy storage devices such as battery. Maximum output power of PV cell can be obtained when coupled with Power Electronics converter. Power Electronic converter is the converter which interfaces sources with the loads along with energy storage devices which are necessary to improve the steady state and dynamic characteristics.

1.2 MOTIVATION

One of the necessity is to switch to TPC is its higher efficiency. The Multiple input converter instead of conventional converters has several advantages such as high efficiency, reduced conversion stages, lower cost, more compact packing, excellent management of power among the ports and provides centralized control. A three-port converter(TPC) consist of an source port connected to an PV source, load connected to an output port and an energy storage device connected to a bidirectional port can be excellently used in renewable power system application. In comparison to isolated TPC, non-isolated TPC has integration level very high and also power

density is quiet high. Power conversion in non-isolated TPC are achieved by combining two individual converters through a common bus. Conventional dc-dc converter cannot be used for hybrid power system application because of their unidirectional power flow capability. This limitation is due to presence of diodes in their circuit diagram which prevents reverse flow of current. Thus there was a need to design a converter which can overcome the limitations of basic dc-dc converter. Bidirectional converter provides as a good candidate for the above problem. By using multiple input multiple output (MIMO) converter we can improve the response of the system.

1.3 CONTRIBUTION OF THE THESIS

The main aim of this paper is to analyze, design and control three port converter. In addition to this, also control power flow in TPC i.e. power flow path in a TPC are fully independent and controllable of each other. Some of the important points of this thesis are:

1. Power flow analysis on the Boost TPC.
2. Designing of a MPPT controller for input voltage regulation (IVR) in order to extract maximum power from PV panel.
3. Output voltage control can be achieved by Output voltage regulation, whereas battery voltage regulation (BVR), battery current regulation (BCR) are employed for maximum voltage and current charging control respectively.
4. Converter circuit design equations for dynamic modelling.

1.4 LITERATURE REVIEW

In order to implement MIC, various dc sources are connected in series and thus output voltage regulation can be achieved.[4]-[5]. The above MICs can operate even if anyone of the sources are not working or failed. In next one, parallel connection of dc buses were done but it's control scheme depends on time- sharing concept due to clamped voltage [12]. Thus, power flow from source to load would not be simultaneous, i.e. one source will be delivering power at a time. For generating MIC, a systematic approach is introduced based on pulsating voltage source cells (PVSCs) and pulsating current source cells (PCSCs) [4]. Various three port converters have been proposed and invented for numerous applications due to their merits, such as stand-alone power system [2], grid power system [1], and fuel-cell [16]. A lot of study has been done in isolated TPC

topology which can be developed through high frequency transformer via magnetic coupling [16]. Non-isolated converter can be available in the form of boost, buck-boost, sepic, etc whereas isolated converter can be available in the form of bridge topologies. The former has compact design and high power density whereas latter has .merits of flexible voltage level but uses high frequency transformer [17]. A isolated topology can be constructed by using primary side of an pulse width modulation (PWM) converter [9]-[10]. Typical configurations of TPC have been found contains a unidirectional converter and a bidirectional converter [17]-[18] but these has a demerit of multiple device sharing and also due to multiple conversion stages suffered from low efficiency. Some multiple-input converters have been proposed having high integration and high power density but power flow is unidirectional [11]-[12].In order to reduce the cost of PV panels, it is mentioned in [14] that converter should track maximum power from the PV panel. Under partially loaded condition in the system, power flowing into battery is very high. If the battery's state of charge (SOC) is high, then power flowing causes battery voltage high. Thus, battery life reduces. So, whenever power flowing in to the battery is very high, then it is suggested [15] to use battery current controller. Thus, they are not useful for bidirectional storage element. So we need to design a converter which is suitable for bidirectional power flow, has higher efficiency and high power density. The present work deals with study of TPC in which power flow among all ports must be simultaneous. In this, DI mode is explained in detail along with its small signal modelling of the converter.

1.5 STRUCTURING OF THE THESIS

- Chapter 2: provides idea about photovoltaic (PV) panel and also describes TPC topology in detail with its all three modes of working along with their steady state analysis.
- Chapter 3: deals with state space analysis and their small signal modelling. It also explains state space averaging method.
- Chapter 4: Modelling and control design are explained in this chapter.
- Chapter 5: In this chapter, simulation results along with conclusion and future task are presented.

CHAPTER 2

THREE PORT DC-DC CONVERTER TOPLOGY & STEADY STATE ANALYSIS

2.1 Overview of Photovoltaic (PV) System

Fig. 2.1 Basic block diagram of PV battery charging system

The above block diagram shows is a basic structure of PV battery charging system. The solar cell also known as photovoltaic cell, which is a semiconductor device which converts solar energy in to electrical energy. The output of PV cell is a dc, so output of PV cell is given to dc-dc converter and the output of converter is connected to the load/battery.

In a PV array, several photovoltaic cells are connected in series and parallel. In order to increase the voltage of the module, series connections of the cells will be preferred whereas for increasing the current, the parallel connection will be preferred. Basically photovoltaic cell is a current source or we can say that it is voltage controlled current source (VCCS). It consist of a diode connected in parallel with current source. Solar cell can be placed above to the ground because we can find leakage current. Now in order to minimize this current we use shunt resistance of high value and we use series resistance also.

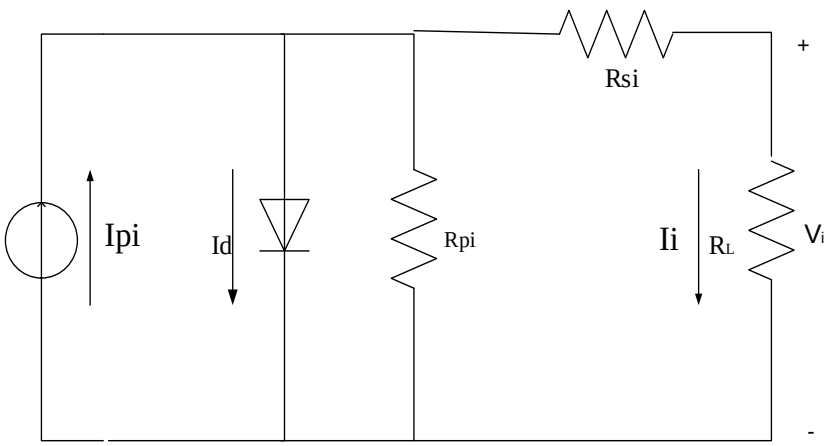

Fig. 2.2 Basic equivalent circuit of photovoltaic (PV) cell

The basic equation of the ideal photovoltaic cell is given by:

$$I_i = I_{pi} - I_o\left[\exp\left(\frac{q*V_i}{\mathrm{b}*k*T}\right)-1\right] \tag{2.1}$$

Where,

I_{pi}= incident light or photon current,

I_o= reverse biased current of diode,

q = charge of electron (1.602*10−19C),

k = Boltzmann constant (1.3806503・10−23J/K),

T = p-n junction temperature in (K), and

b = ideality factor of diode.

The equation (2.1) of basic PV cell does not represent practical PV cell characteristics. Thus we can write equation (2.1) as

$$I_i = I_{pi} - I_o\left[\exp\left(\frac{V_i + R_{si}I_i}{V_t b}\right)-1\right] - \frac{V_i + R_{si}I_i}{R_{pi}} \tag{2.2}$$

Maximum power point voltage (V_{mppt})	40.00
Maximum power point current (I_{mppt})	3.00
Open circuit voltage (V_{oc})	50.00
Short circuit current (I_{sc})	3.90

No. of cells in series (N_s)	60
No. of cells in parallel(N_p)	1

Table 2.1 Electrical Characteristics of PV Module

The I-V characteristics basically depends on ambient temperature and insolation. In the below characteristic, the open circuit voltage (V_{OC}) and current (I_{SC})are mentioned at the two end points. By knowing this voltage and current we can easily calculate power from this curve. The power at open and short circuit conditions are always zero and at maximum power point we can maximum power. The power curve is shown below.

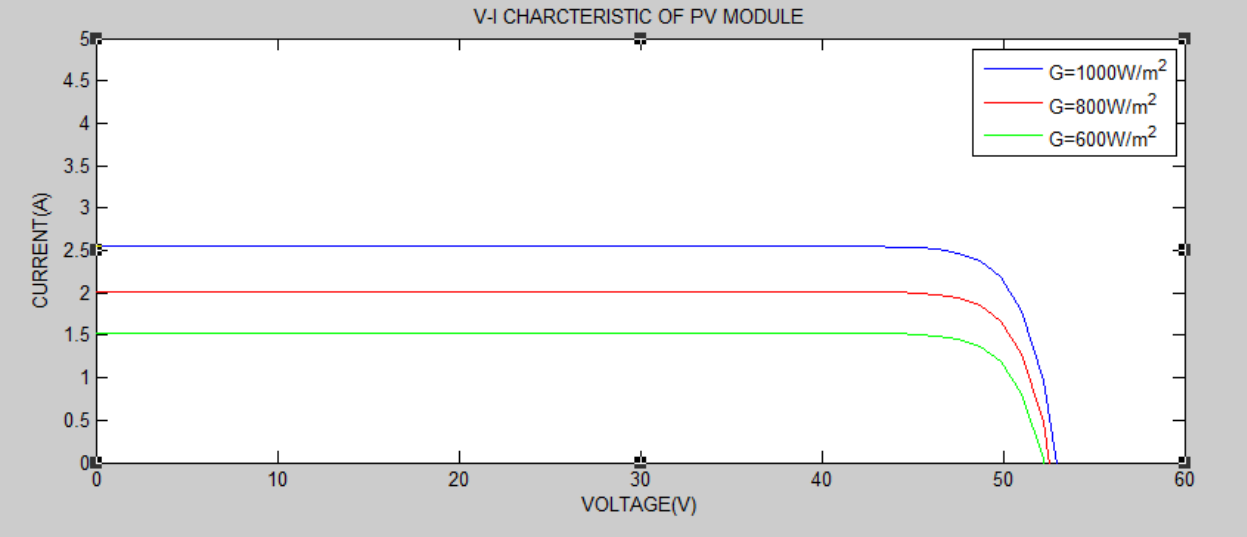

Fig. 2.3 V-I characteristic of PV at different insolation

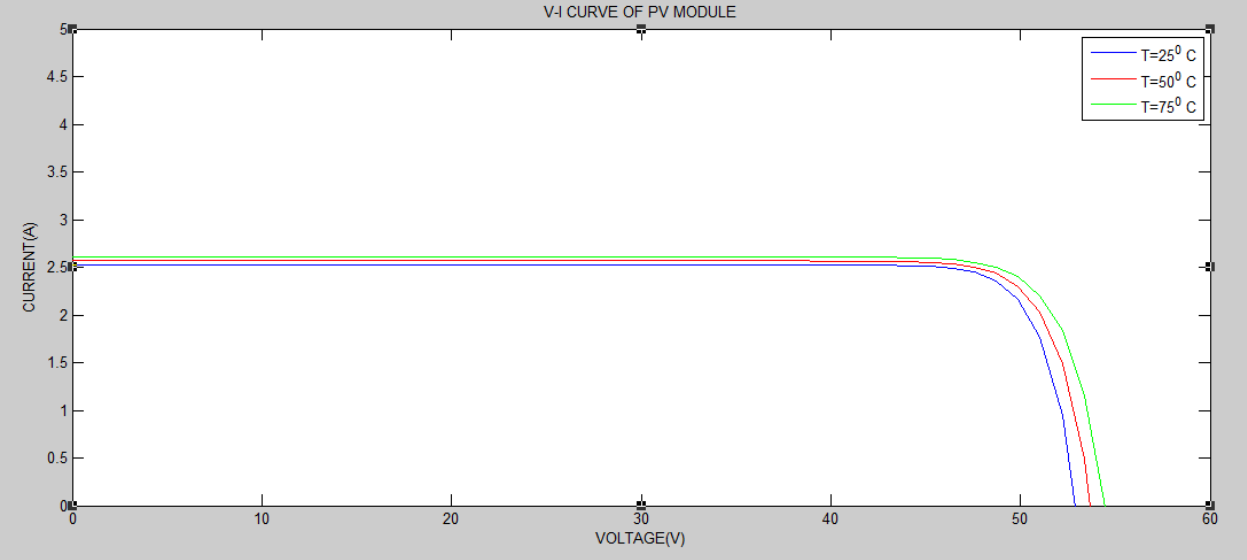

Fig. 2.4 V-I characteristic of PV at different temperature

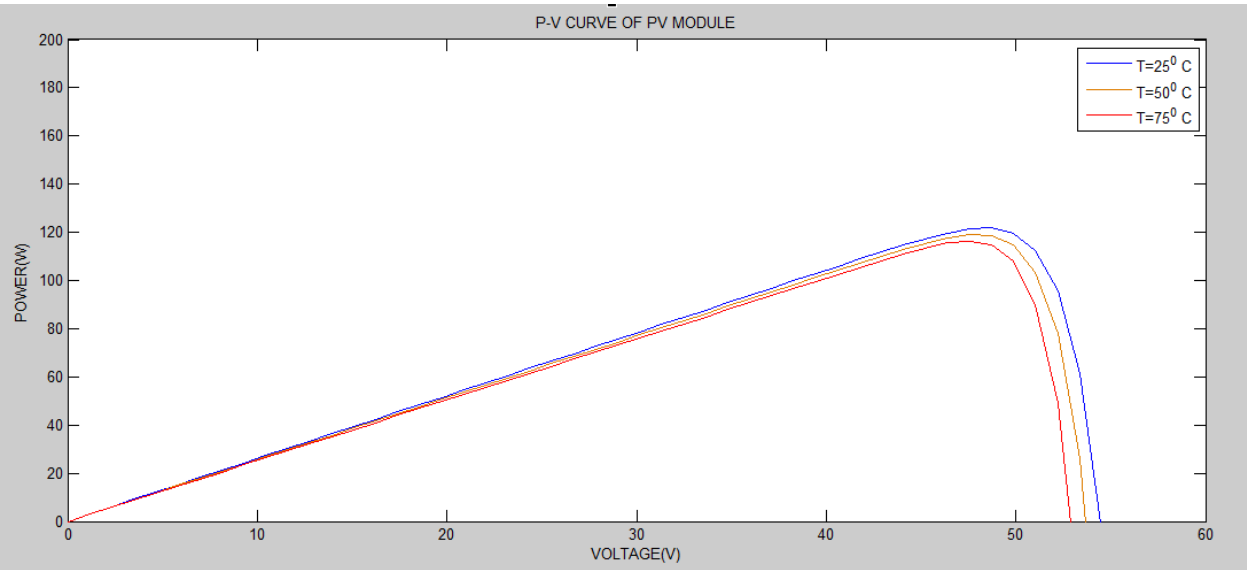

Fig. 2.5 P-V characteristic of PV at different insolation

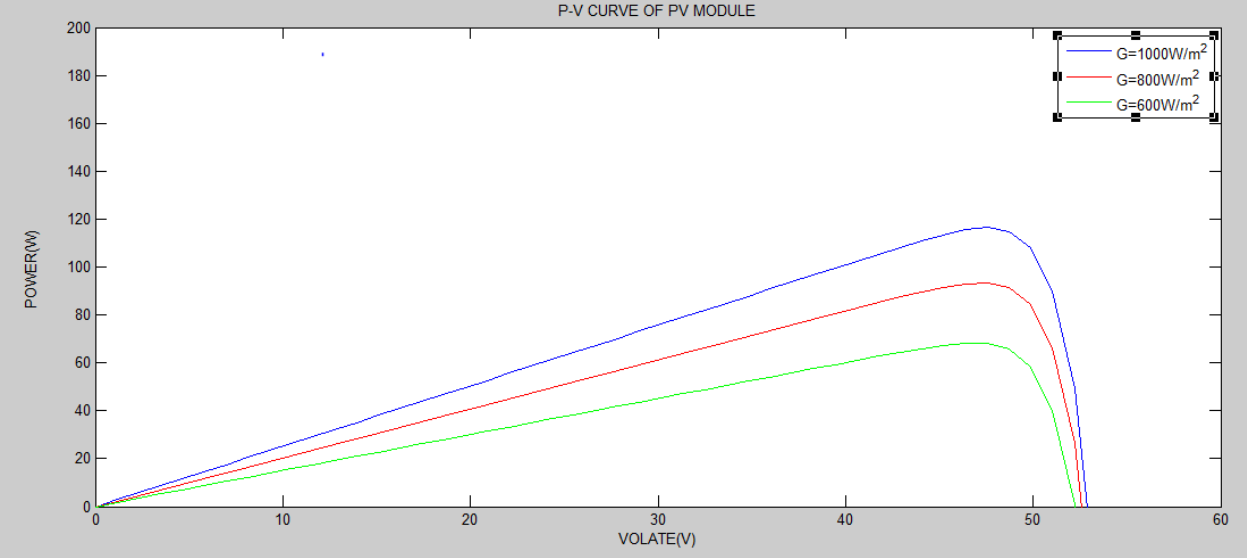

Fig. 2.6 P-V characteristic of PV at different temperature

2.2 THREE PORT CONVERTER TOPOLOGY

A TPC synthesis is analyzed by the means of DIC and DOC by building an additional power flow path. When both PV panel and battery is supplying power to load then TPC act as dual input converter. Similarly, when both load and battery drawing power from the panel then TPC act as dual output converter. Let us consider p_i, p_{out}, p_{bat} as input power, output power and battery power respectively such that,

$$p_i = p_{bat} + p_{out}$$

Basically TPC can work on three different modes depending on the input-output power relationship.

- Dual- Input (DI) Mode- during this mode battery and PV panel together act as a source i.e. battery is in discharging mode to support load along with PV source. In this mode $p_i < p_{out}$.

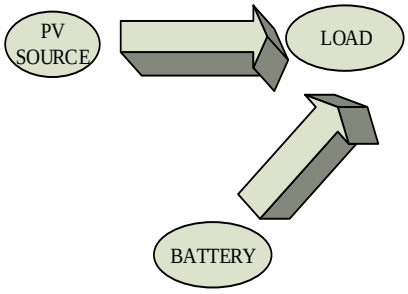

Fig. 2.7 DI MODE

Dual- Output (DO) Mode- during this mode both battery and load is extracting power from PV source i.e. source is supplying power to load and battery is absorbing excess power. Here, $p_i \geq p_{out}$.

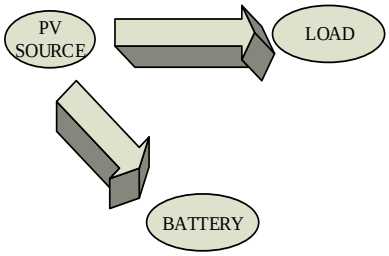

Fig. 2.8 DO MODE

Single-Input Single-Output (SISO) Mode- here battery alone is supplying power to the load. Here, $p_i = 0$.

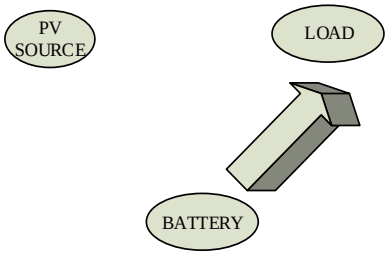

Fig. 2.9 SISO MODE

On combining all the three modes we get three port converter (TPC) and all the power flow paths are independent of each other and controllable.

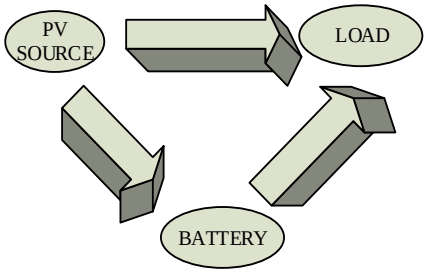

Fig. 2.10 Full graph of TPC

2.3 ANALYSIS OF THE BOOST-TPC

In a Boost-TPC as mentioned in [1], conventional boost converter are merged such that $V_i < V_b < V_L$ for all flow of power from V_i to V_{bi}, V_i to V_L, V_{bi} to V_o. In the below fig.2, filter capacitors C_i and C_{bi} are used to smooth pulsating currents. Vs1, Vs2 and Vs3 are PWM signals with D1, D2 and D3 are the duty cycle of switches S1, S2 and S3, respectively.

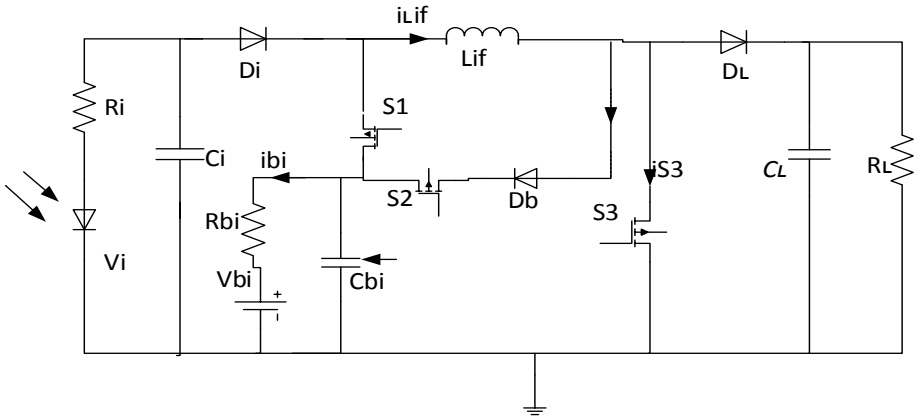

Fig. 2.11 Equivalent circuit of Boost-TPC

The operational principle of three modes of TPC are discussed below:

2.3.1 DI Mode

Small signal approximation replaces waveforms with their low frequency averaged values. By doing small signal analysis, we can transform non-linear equations in to linear equations. Thus, to obtain linearized model for any non-linear device, we can perform small signal modelling.

In DI mode, four switching states are possible in one time period [1].

State 1: S_1 is ON and S_3 is ON. L_{if} sinks energy from $V_{bi}$and I_{Lif}increases.

$$V_{lif}(t) = Lif\,\frac{di_{lif}(t)}{dt} = \left\langle V_{cbi}(t)\right\rangle_{Ts} \tag{2.3}$$

State 2: S_3 is ON and S_1 is OFF. L_{if} sinks energy from $V_{in}$and I_{Lif}increases.

$$V_{lif}(t) = Lif\,\frac{di_{lf}(t)}{dt} = \left\langle V_{ci}(t)\right\rangle_{Ts} \tag{2.4}$$

State 3: S_1 is OFF and S_3 is ON. V_o is powered by both V_{bi} and L_{if} (releasing energy), and

$$V_{lif}(t) = Lif\,\frac{di_{lif}(t)}{dt} = \left\langle V_{cbi}(t)\right\rangle_{Ts} - \left\langle V_{L}(t)\right\rangle_{Ts} \tag{2.5}$$

State 4: S_1 and S_3 both OFF. V_o is powered by both V_i and L_{if} (releasing energy), and I_{Lif}decreases.

$$V_{lif}(t) = Lif\,\frac{di_{lif}(t)}{dt} = \left\langle V_{ci}(t)\right\rangle_{Ts} - \left\langle V_{L}(t)\right\rangle_{Ts} \tag{2.6}$$

For a DI mode

During steady state, applying inductor volt-second balance on Lif inductor we get:

$$\left\langle V_{lif}\right\rangle_{T_s} = V_{cbi}D_1T_S + V_{ci}(D_3 - D_1)T_S + (V_{ci} - V_L)(1 - D_3)T_S = 0 \tag{2.7}$$

So, equation (2.5) has been solved and written as

$$V_L = \frac{V_{ci}(1 - D_1) + V_{cbi}D_1}{(1 - D_3)} \tag{2.8}$$

Thus, from equation (2.8) we can observe that if D_3 tends to 1 then, the gain of the converter or the output voltage becomes infinity. So the above TPC can act as conventional boost converter.

By analyzing states 1 to 4, we can say that the regulation of output voltage can be done by D_1 while the power shared by PV panel and battery is regulated by D_3 or MPPT can be used to regulate input.

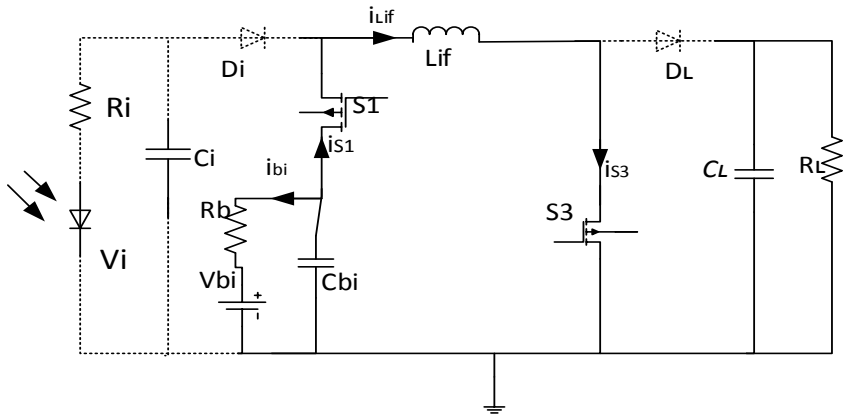

Fig. 2.12 Equivalent states of DI mode: State 1

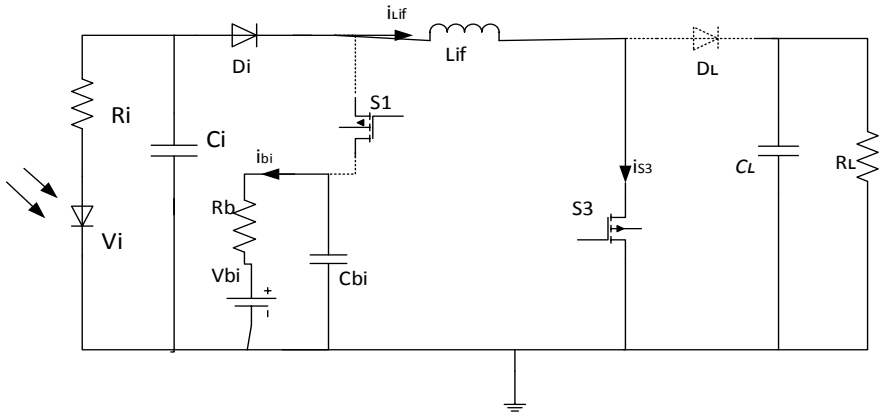

Fig. 2.13 Equivalent states of DI mode: State 2

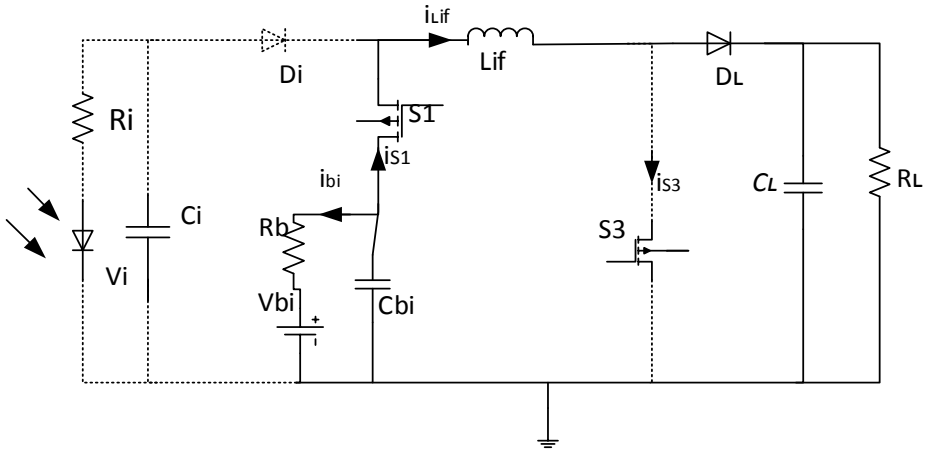

Fig. 2.14 Equivalent states of DI mode: State 3

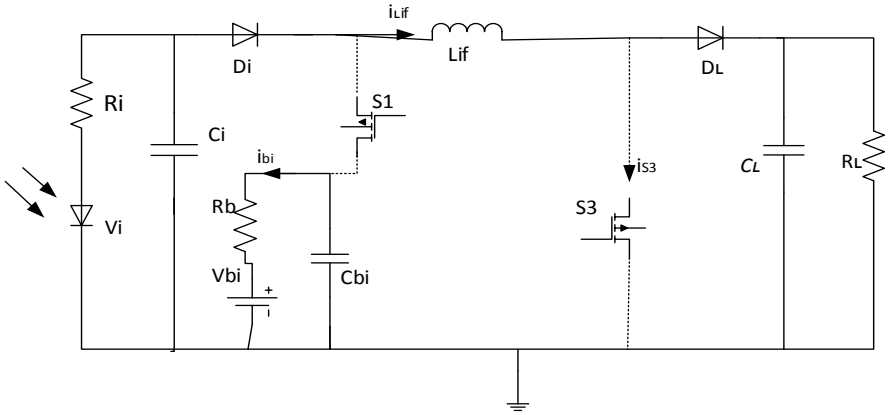

Fig. 2.15 Equivalent states of DI mode: State 4

DI mode works under 2 different condition:

1. $\mathbf{D_3 > D_1}$- In this mode, inductor L_{if} is sinking energy from both battery and PV source but load is powered by only PV source. Thus, we can inferred that in this case inductor was charging for more time.

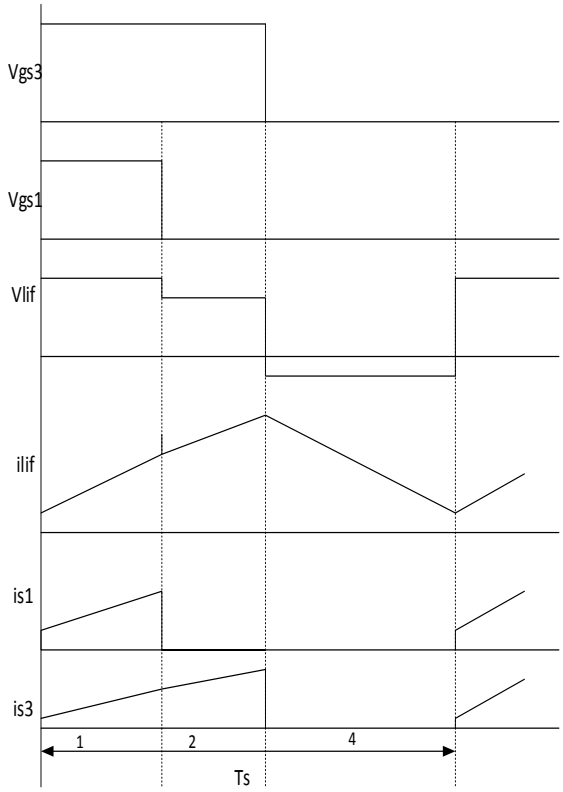

Fig. 2.16 Waveforms for the Boost-TPC in DI mode when $D_3 > D_1$

2. $\mathbf{D_1 > D_3}$- In this mode, inductor L_{if} is sinking energy from battery alone and now load is powered by both battery and PV source. Thus, in this case inductor was charging for less time rather than releasing energy to load for more time

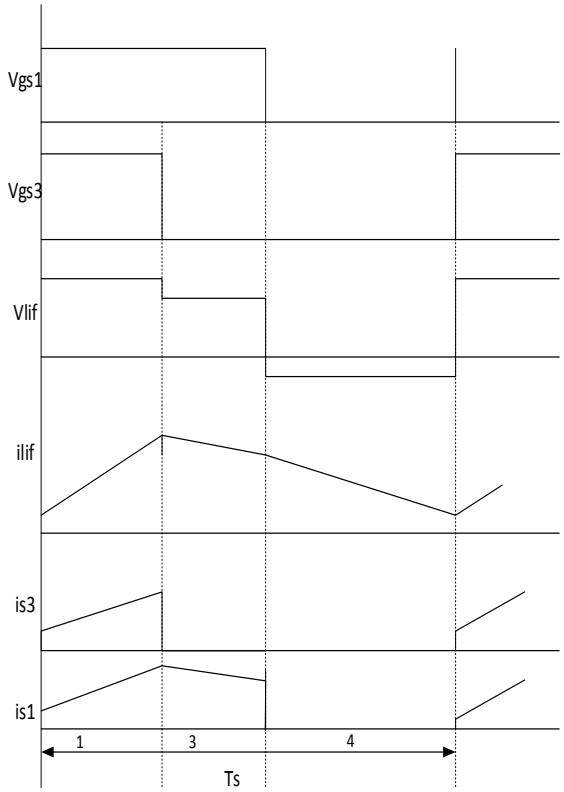

Fig. 2.17 Waveforms for the Boost-TPC in DI mode when $D_1 > D_3$

2.3.2 DO Mode

In DO Mode, three switching states are possible in one switching period [1].

State 1: S_3 is ON and S_2 is OFF. L_{if} sinks energy from V_{in} and I_{Lif} increases

$$V_{lif}(t) = Lif\ \frac{d_{i_{lif}}(t)}{dt} = \langle V_{ci}(t) \rangle_{Ts} \tag{2.9}$$

State 2: S_3 is OFF and S_2 is ON. V_{bi} is energized by both V_i and L_{if} (releasing energy), and

$$V_{lif}(t) = Lif\ \frac{d_{i_{lif}}(t)}{dt} = \langle V_{ci}(t) \rangle_{Ts} - \langle V_{bi}(t) \rangle_{Ts} \tag{2.10}$$

State 3: S_3 is OFF and S_2 *is OFF*. V_L *is* energized by both V_i and L_{if} (releasing energy), and

$$V_{lif}(t) = Lif\ \frac{d_{i_{lif}}(t)}{dt} = \langle V_{ci}(t) \rangle_{Ts} - \langle V_L(t) \rangle_{Ts} \tag{2.11}$$

For a DO mode

During steady state, applying inductor volt-second balance on Lif inductor we get:

$$V_L = \frac{V_i - V_{bi} D_2}{1 - D_3 - D_2} \tag{2.12}$$

Thus from the above equation it is clearly visible that as D_1 becomes 1 and D_2 becomes zero, then both V_{bi} and V_L becomes infinity. Thus, gain in the DO mode of Boost-TPC is comparable to conventional boost converter.

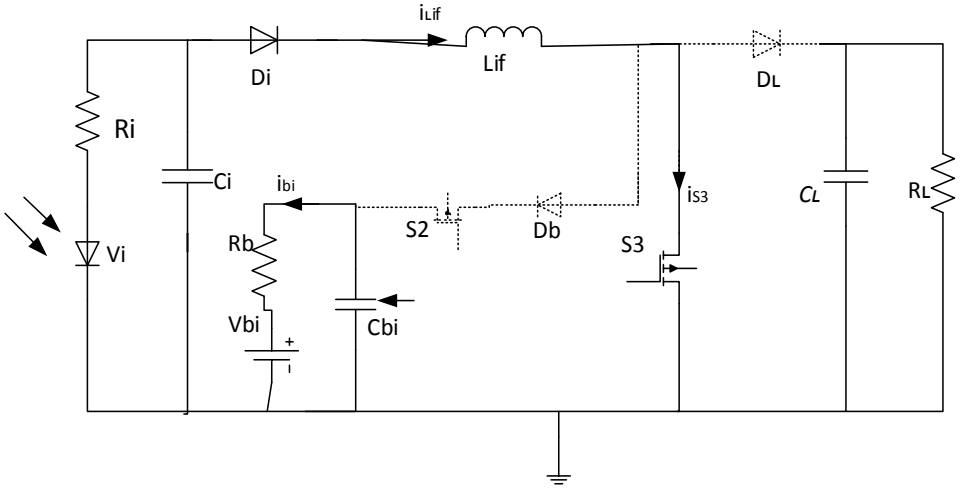

Fig. 2.18 Equivalent states of DO mode: State 1

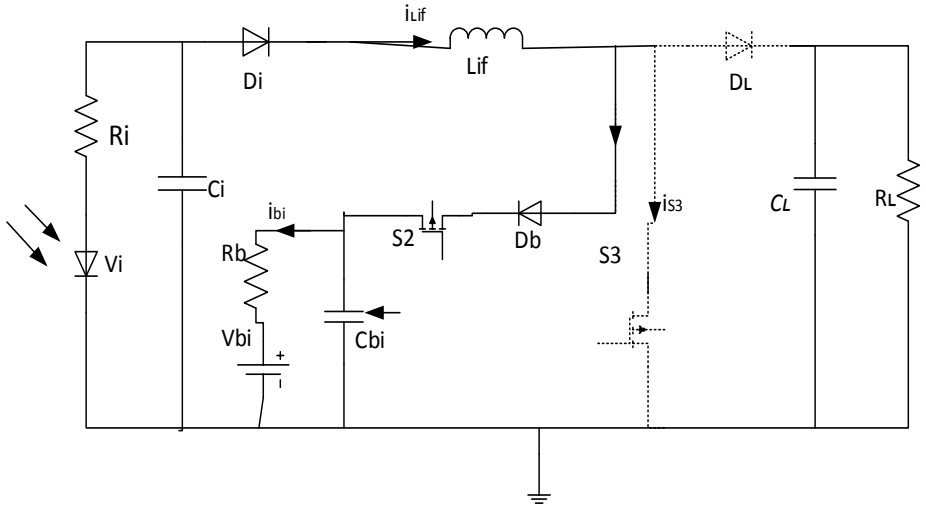

Fig. 2.19 Equivalent states of DO mode: State 2

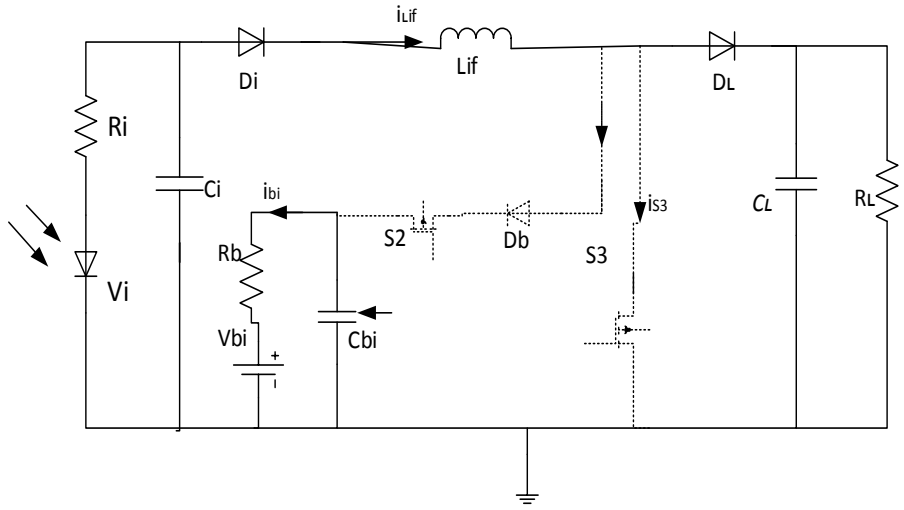

Fig. 2.20 Equivalent states of DO mode: State 3

2.3.3 SISO Mode

In this mode, S_2 is OFF and S_1 is ON. In this mode, Boost-TPC acts as a conventional boost converter.

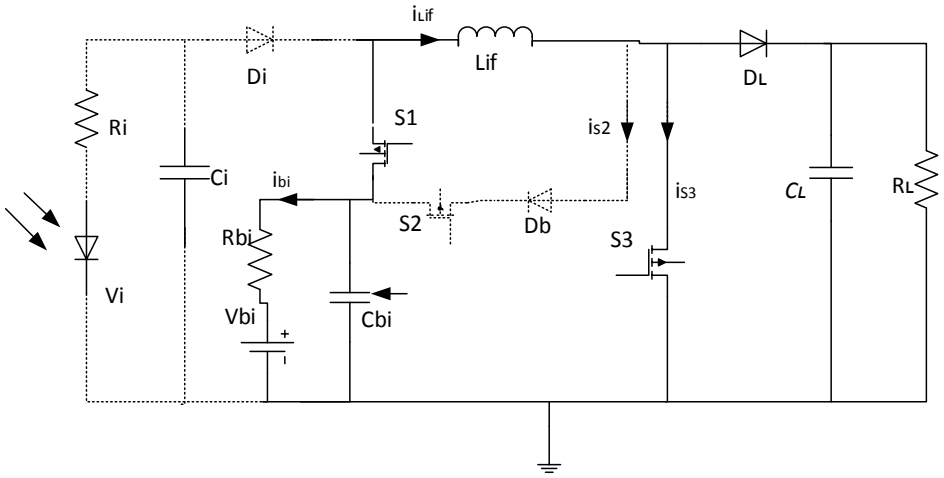

Fig. 2.21 Equivalent circuit Boost-TPC in SISO mode

CHAPTER 3

STATE SPACE ANALYSIS AND AVERAGING TECHNIQUES

3.1 INTRODUCTION

In this chapter, small signal modelling is described and the parameters of the circuits are introduced. In order to design optimized controller, small signal modelling plays a very important role. TPC is a multiport converter and such converter is high order system. For multiport converter, it is very tedious to get converter dynamics. Thus, there is a need to design such a model which will not only optimize converter dynamics but also helps in realizing closed-loop control. General Boost-TPC works in three different modes. Out of the three available modes, dual-input (DI) mode has been explained in detail along with its dynamic modelling. DI mode has four states in one switching cycle. In order to design optimized controller, small signal modelling plays a very important role. Thus small signal model for DI mode is derived. For a DI mode, both PV source and battery acts as a source and power is delivered to the load. The PV panel voltage V_i and the battery voltage V_{bi} together constitutes the voltage sources. The TPC consist of four energy storage element and state equation has been developed for each stage. By using these equations, small signal transfer function of the TPC are developed. TPC consist of an inductor L_{if}, PV panel capacitor C_i, battery capacitor C_{bi} and the load capacitor C_L. Internal resistance of the inductor and the on time resistance of the MOSFET are neglected. The internal resistances for the panel source and the battery source are given as R_i and R_{bi}, respectively. The load voltage and the load resistance are given as V_L and R_L, respectively.

3.2 STATE SPACE EQUATION

As we have discussed already about the DI mode working in chapter 2, so we can derived state space equation for each state individually. The below diagram shows the Boost-TPC working in DI mode.

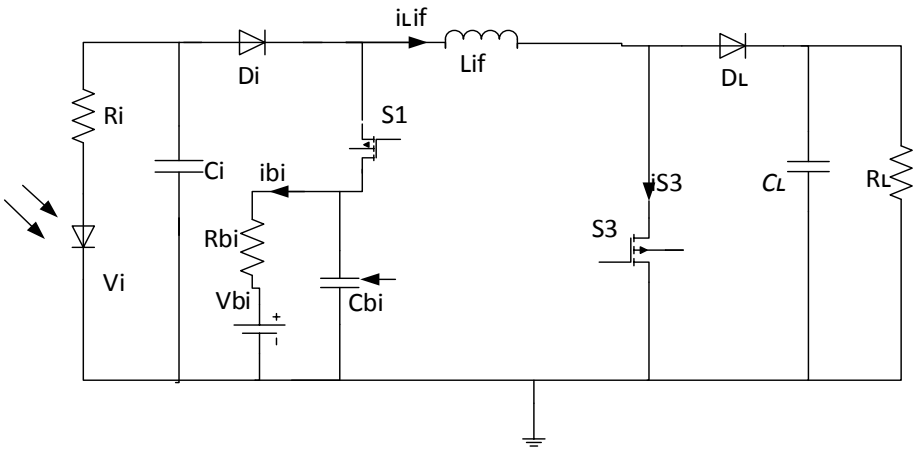

Fig. 3.1 Equivalent circuit of Boost-TPC in DI mode

State 1: S_1 is ON and S_3 is ON. L_{if} sinks energy from $V_{bi}$and I_{Lif}increases.

The voltage across the inductor L_{if} is given by

$$V_{Lif}(t) = Lif\,\frac{dI_{Lif}(t)}{dt} = V_{Ci}(t) \tag{3.1}$$

The current across the capacitor C_i and C_{bi} is given by

$$I_{CL}(t) = \frac{C_L dV_L(\mathrm{t})}{dt} = \frac{V_L(t)}{R_L} \tag{3.2}$$

$$I_{Cbi}(t) = \frac{C_{bi} dV_{Cbi}(t)}{dt} = \frac{V_{Cbi}(t) - V_{bi}(t)}{R_{bi}} + I_{Lif}(t) \tag{3.3}$$

Therefore for the State 1, state space equation is given by:

$$\begin{aligned} \dot{X}_T &= A_{11}X_T + B_{11}U \\ Y &= C_{11}X_T + E_{11}U \end{aligned} \tag{3.4}$$

Where

$$X_T = \begin{bmatrix} I_{Lif} \\ V_L \\ V_{Ci} \\ V_{Cbi} \end{bmatrix},\ U = \begin{bmatrix} V_i \\ V_{bi} \end{bmatrix}$$

$$A_{11} = \begin{bmatrix} 0 & 0 & 0 & \frac{1}{Lif} \\ 0 & \frac{1}{R_L C_L} & 0 & 0 \\ 0 & 0 & 0 & 0 \\ \frac{1}{C_{bi}} & 0 & 0 & \frac{1}{R_{bi} C_{bi}} \end{bmatrix},\ B_{11} = \begin{bmatrix} 0 & 0 \\ 0 & 0 \\ 0 & 0 \\ 0 & \frac{-1}{R_{bi} C_{bi}} \end{bmatrix}$$

$$C_{11} = \begin{bmatrix} 0 & 0 & 0 & 1 \end{bmatrix},\ E_{11} = \begin{bmatrix} 0 & 0 \\ 0 & 0 \\ 0 & 0 \\ 0 & 0 \end{bmatrix}$$

State 2: S_3 is ON and S_1 is OFF. L_{if} sinks energy from $V_{in}$and I_{Lif}increases.

The voltage across the inductor L_{if} is given by

$$V_{Lif}(t) = Lif \frac{dI_{Lif}(t)}{dt} = V_{Ci}(t) \tag{3.5}$$

The current across the capacitor C_i and C_{bi} is given by

$$I_{CL}(t) = \frac{C_L dV_L(t)}{dt} = \frac{V_L(t)}{R_L} \tag{3.6}$$

$$I_{Ci}(t) = \frac{C_i dV_{Ci}(t)}{dt} = \frac{V_i(t) - V_{ci}(t)}{R_i} + I_{Lif}(t) \tag{3.7}$$

$$I_{Cbi}(t) = \frac{C_{bi} dV_{Cbi}(t)}{dt} = \frac{V_{cbi}(t) - V_{bi}(t)}{R_{bi}} \tag{3.8}$$

Therefore for the State 2, state space equation is given by

$$\begin{aligned} \dot{X}_T &= A_{21}X_T + B_{21}U \\ Y &= C_{21}X_T + E_{21}U \end{aligned} \tag{3.9}$$

Where

$$A_{21} = \begin{bmatrix} 0 & 0 & \frac{1}{Lif} & 0 \\ 0 & \frac{1}{R_L C_L} & 0 & 0 \\ \frac{1}{C_i} & 0 & \frac{-1}{R_i C_i} & 0 \\ 0 & 0 & 0 & \frac{1}{R_{bi} C_{bi}} \end{bmatrix}, \; B_{21} = \begin{bmatrix} 0 & 0 \\ 0 & 0 \\ \frac{1}{R_i C_i} & 0 \\ 0 & \frac{-1}{R_{bi} C_{bi}} \end{bmatrix}$$

$$C_{21} = \begin{bmatrix} 0 & 0 & 0 & 1 \end{bmatrix}, \; E_{21} = \begin{bmatrix} 0 & 0 \\ 0 & 0 \\ 0 & 0 \\ 0 & 0 \end{bmatrix}$$

State 3: S_1 is OFF and S_3 is ON. V_o is powered by both V_{bi} and L_{if} (releasing energy), and

The voltage across the inductor L_{if} is given by

$$V_{lif}(t) = Lif \frac{di_{lif}(t)}{dt} = V_{cbi}(t) - V_L(t) \tag{3.10}$$

The current across the capacitor C_i and C_{bi} is given by

$$I_{CL}(t) = \frac{C_L dV_L(t)}{dt} = \frac{V_L(t)}{R_L} - I_{Lif}(t) \tag{3.11}$$

$$I_{Cbi}(t) = \frac{C_{bi} dV_{Cbi}(t)}{dt} = \frac{V_{cbi}(t) - V_{bi}(t)}{R_{bi}} + I_{Lif}(t) \tag{3.12}$$

Therefore for the State 3, state space equation is given by

$$\begin{aligned} \dot{X}_T &= A_{31}X_T + B_{31}U \\ Y &= C_{31}X_T + E_{31}U \end{aligned} \tag{3.13}$$

Where

$$A_{31}=\begin{bmatrix} 0 & \frac{-1}{Lif} & 0 & \frac{1}{Lif} \\ \frac{1}{C_L} & \frac{1}{R_L C_L} & 0 & 0 \\ 0 & 0 & 0 & 0 \\ \frac{1}{C_{bi}} & 0 & 0 & \frac{1}{R_{bi}C_{bi}} \end{bmatrix},\ B_{31}=\begin{bmatrix} 0 & 0 \\ 0 & 0 \\ 0 & 0 \\ 0 & \frac{-1}{R_{bi}C_{bi}} \end{bmatrix}$$

$$C_{31}=\begin{bmatrix} 0 & 0 & 0 & 1 \end{bmatrix}, E_{31}=\begin{bmatrix} 0 & 0 \\ 0 & 0 \\ 0 & 0 \\ 0 & 0 \end{bmatrix}$$

State 4: S_1 and S_3 both OFF. V_o is powered by both V_i and L_{if} (releasing energy), and I_{Lif} decreases.

The voltage across the inductor L_{if} is given by

$$V_{Lif}(t)=Lif\frac{di_{Lif}(t)}{dt}=V_{ci}(t)-V_L(t) \tag{3.14}$$

The current across the capacitor C_i and C_{bi} is given by

$$I_{CL}(t)=\frac{C_L dV_L(t)}{dt}=\frac{V_L(t)}{R_L}-I_{Lif}(t) \tag{3.15}$$

$$I_{Ci}(t)=\frac{C_i dV_{Ci}(t)}{dt}=\frac{V_i(t)-V_{ci}(t)}{R_i}+I_{Lif}(t) \tag{3.16}$$

$$I_{Cbi}(t)=\frac{C_{bi} dV_{Cbi}(t)}{dt}=\frac{V_{cbi}(t)-V_{bi}(t)}{R_{bi}} \tag{3.17}$$

Therefore for the State 4, state space equation is given by:

$$\begin{aligned} \dot{X}_T &= A_{41}X_T + B_{41}U \\ Y &= C_{41}X_T + E_{41}U \end{aligned} \tag{3.18}$$

Where

$$A_{41}=\begin{bmatrix} 0 & \frac{-1}{Lif} & \frac{1}{Lif} & 0 \\ \frac{1}{C_L} & \frac{1}{R_L C_L} & 0 & 0 \\ \frac{1}{C_i} & 0 & \frac{-1}{R_i C_i} & 0 \\ 0 & 0 & 0 & \frac{1}{R_{bi} C_{bi}} \end{bmatrix},\ B_{41}=\begin{bmatrix} 0 & 0 \\ 0 & 0 \\ \frac{1}{R_i C_i} & 0 \\ 0 & \frac{-1}{R_{bi} C_{bi}} \end{bmatrix}$$

$$C_{41}=\begin{bmatrix} 0 & 0 & 0 & 1 \end{bmatrix}, E_{41}=\begin{bmatrix} 0 & 0 \\ 0 & 0 \\ 0 & 0 \\ 0 & 0 \end{bmatrix}$$

3.3 State Space Modelling

1- $\mathbf{D_3 > D_1}$

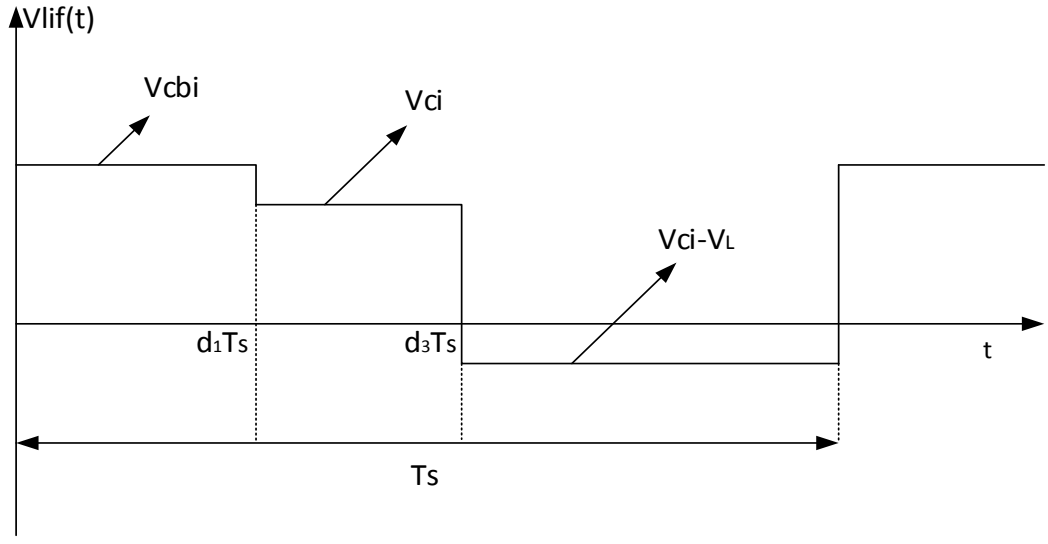

Fig. 3.2 Waveform of inductor voltage at $D_3 > D_1$

Linearized converter equation as

$$L_{if}\frac{d[\hat{i}_{Lif}(t)]}{dt}=\mathrm{D}_1\hat{\mathrm{v}}_{cbi}(\mathrm{t})+\hat{v}_{ci}(t)[1-\mathrm{D}_1]+[\mathrm{V}_{cbi}(t)-V_{ci}(t)]\hat{\mathrm{d}}_1(\mathrm{t})-\hat{v}_L(t)[1-\mathrm{D}_3]+V_L\,\hat{\mathrm{d}}_1(\mathrm{t}) \quad (3.19)$$

$$C_L\frac{d[\hat{v}_L(t)]}{dt}=I_{Lif}\,\hat{\mathrm{d}}_3(\mathrm{t})-\hat{i}_{Lif}(t)[1-\mathrm{D}_3] \quad (3.20)$$

$$C_{bi}\frac{d[\hat{v}_{cbi}(t)]}{dt}=\hat{\mathrm{d}}_1(\mathrm{t})I_{Lif}+\hat{i}_{Lif}(t)\,\mathrm{D}_1+\left[\frac{\hat{\mathrm{v}}_{cbi}(\mathrm{t})-\hat{\mathrm{v}}_{bi}(\mathrm{t})}{R_{bi}}\right] \quad (3.21)$$

$$C_i\frac{d[\hat{v}_i(t)]}{dt}=\left(\frac{\hat{\mathrm{v}}_i(\mathrm{t})-\hat{\mathrm{v}}_{ci}(\mathrm{t})}{R_i}\right)[1-\mathrm{D}_1]+\hat{i}_{Lif}(t)[1-\mathrm{D}_1]-\hat{\mathrm{d}}_1(\mathrm{t})\left[\left(\frac{V_i(\mathrm{t})-V_{ci}(\mathrm{t})}{R_i}\right)+I_{Lif}\right] \quad (3.22)$$

2-$\mathbf{D_1 > D_3}$

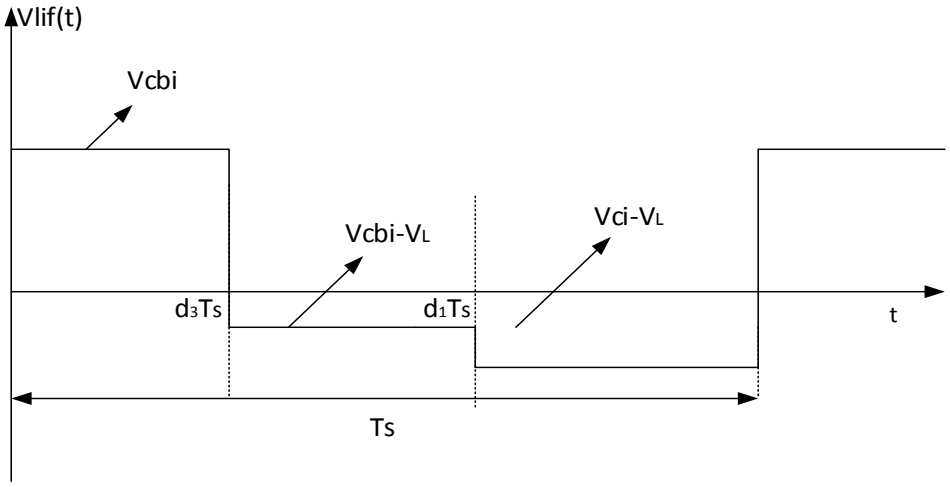

Fig. 3.3 Waveform of inductor voltage at $D_1 > D_3$

Converter averaged equations are given as

$$V_{Lif}(t)=V_{cbi}(t)d_3(t)+[V_{cbi}(t)-V_L(t)[\mathrm{d}_1(t)-d_3(t)]+[\mathrm{V}_{cin}(t)-V_L(\mathrm{t})][1-\mathrm{d}_1(t)] \quad (3.23)$$

$$I_{CL}(t)=\left(\frac{V_L(\mathrm{t})}{R_L}\right)d_3(t)+\left(\frac{V_L(\mathrm{t})}{R_L}-I_{Lif}(t)\right)[1-\mathrm{d}_1(\mathrm{t})] \quad (3.24)$$

$$I_{cbi}(t)=\left[\left(\frac{V_{cbi}(t)-V_{bi}(t)}{R_{bi}}\right)+I_{Lif}(t)\right]d_1(t)+\left(\frac{V_{cbi}(t)-V_{bi}(t)}{R_{bi}}\right)\left[1-d_1(t)\right] \quad (3.25)$$

$$I_{cin}(t) = \left[\left(\frac{V_i(t) - V_{ci}(t)}{R_s} \right) + I_{Lif}(t) \right] [1 - \mathrm{d}_1(\mathrm{t})] \tag{3.26}$$

3.4 State Space Averaging

The use of averaging technique in state space is that it approximates converter non-linear system. Then, linearization of non-linear systems are done about its quiescent point in order to obtain linear time invariant system. The equation for the state space can be given as:

$$\begin{aligned} \dot{X}_T &= A_T X_T + B_T U \\ Y &= C_T X + E_T U \end{aligned} \tag{3.27}$$

The state space equations of the four states of the DI mode are averaged with respect to interval of switching period.

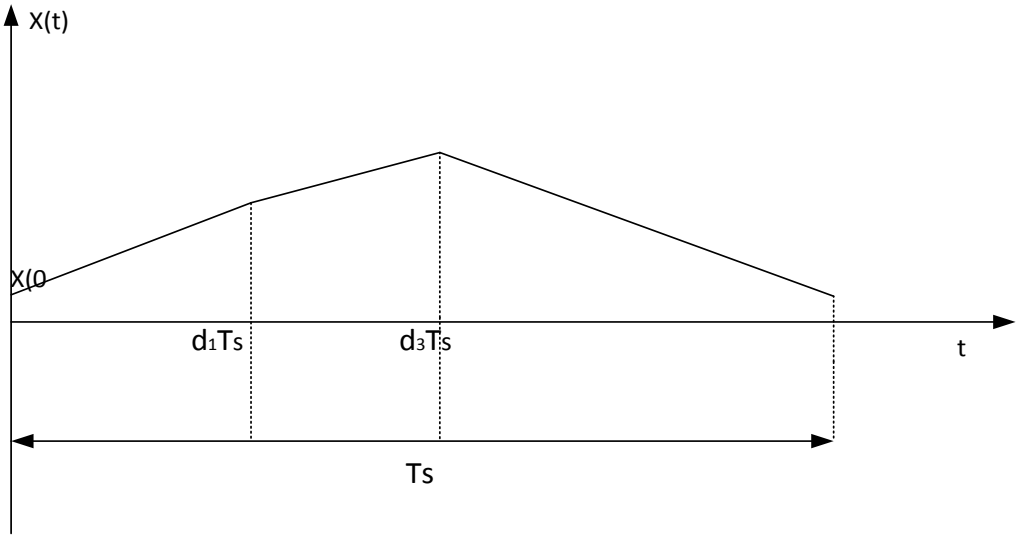

Fig. 3.4 State space waveform

$$X_T(T_S) = X_T(0) + \mathrm{d}_1 T_S[\mathrm{A}_{11} X_T(\mathrm{t}) + \mathrm{B}_{11} U(t)] + [\mathrm{d}_3(t) - \mathrm{d}_1(t)][\mathrm{A}_{21} X_T(\mathrm{t}) + \mathrm{B}_{21} U(t)] + [1 - \mathrm{d}_3(t)][\mathrm{A}_{41} X_T(\mathrm{t}) + \mathrm{B}_{41} U(t)] \tag{3.28}$$

Where

$$\dot{X}_T(t) = \frac{X_T(\mathrm{T}_S) - \mathrm{X}_T(0)}{T_S} \tag{3.29}$$

Therefore, equation (3.28) can be changed to

$$\dot{X}_T(t) = [d_3(t)(A_{21} - A_{31}) + d_1(t)(A_{11} - A_{21}) + A_{31}]X_T(t) + [d_3(t)(B_{21} - B_{31}) + d_1(t)(B_{11} - B_{21}) + B_{31}]U(t) \quad (3.30)$$

Let,

$$\begin{aligned} \dot{X}_T(t) &= \dot{X}_T + \dot{\hat{x}}_T(t) \\ X_T(t) &= X_T + \hat{x}_T(t) \\ U(t) &= U + \hat{u}(t) \\ d_1(t) &= D_1 + \hat{d}_1(t) \\ d_3(t) &= D_3 + \hat{d}_3(t) \end{aligned}$$

The averaged state equation (3.30) can be written as

$$\begin{aligned} &\dot{X}_T + \dot{\hat{x}}_T(t) = [(D_3 + \hat{d}_3(t))(A_{21} - A_{31}) + (D_1 + \hat{d}_1(t))(A_{11} - A_{21}) + A_{31}][X_T + \hat{x}_T(t)] \\ &+[(D_3 + \hat{d}_3(t))(B_{21} - B_{31}) + (D_1 + \hat{d}_1(t))(B_{11} - B_{21}) + B_{31}][U + \hat{u}(t)] \end{aligned} \quad (3.31)$$

Neglecting dc terms and second order terms on both the sides of the equations (3.31), we get

$$\begin{aligned} \dot{\hat{x}}_T &= [D_3(A_{21} - A_{31}) + D_1(A_{11} - A_{21}) + A_{31}]\hat{x}_T(t) + [D_3(B_{21} - B_{31}) + D_1(B_{11} - B_{21}) + B_{31}]\hat{u}(t) \\ &+[(A_{21} - A_{31})X_T + (B_{21} - B_{31})U]\hat{d}_3(t) + [(A_{11} - A_{21})X_T + (B_{11} - B_{21})U]\hat{d}_1(t) \end{aligned} \quad (3.32)$$

Where,

$\hat{x}_T$=perturb small signal (ac) state vector

$\hat{u}$= perturb small signal (ac) input vector

$\hat{d}$= perturb small signal (ac) duty cycle

The state spaceaveraged model that describes converter in equillibrium is

$$\begin{aligned} 0 &= A_T X_T + B_T U \\ Y &= C_T X_T + E_T U \end{aligned} \quad (3.33)$$

The dc components of the state space in steady state are

X_T = dc state vector

U = dc input vector

Y = dc output vector

Where averaged matrices are

$$A_T = D_3\left(A_{21-}A_{31}\right) + D_1\left(A_{11-}A_{21}\right) + A_{31}$$
$$B_T = D_3\left(B_{21-}B_{31}\right) + D_1\left(B_{11-}B_{21}\right) + B_{31}$$
$$C_T = D_3\left(C_{21-}C_{31}\right) + D_1\left(C_{11-}C_{21}\right) + C_{31}$$
$$E_T = D_3\left(E_{21-}E_{31}\right) + D_1\left(E_{11-}E_{21}\right) + E_{31}$$

At steady state, state and output vector are given as

$$X_T = -A_T^{-1}B_T U$$
$$Y = \left(-C_T A_T^{-1}B_T + E_T\right)U \tag{3.34}$$

Where,

$$A_T = \begin{bmatrix} 0 & \frac{-(1-D_3)}{L_{if}} & \frac{(1-D_1)}{L_{if}} & \frac{D_1}{L_{if}} \\ \frac{-(1-D_3)}{C_L} & \frac{1}{R_L C_L} & 0 & 0 \\ \frac{-(1-D_1)}{C_i} & 0 & \frac{(1-D_1)}{C_i} & 0 \\ \frac{D_1}{C_{bi}} & 0 & 0 & \frac{1}{R_{bi}C_{bi}} \end{bmatrix},\ B_T = \begin{bmatrix} 0 & 0 \\ 0 & 0 \\ \frac{1-D_1}{R_{bi}C_{bi}} & 0 \\ 0 & \frac{-1}{R_{bi}C_{bi}} \end{bmatrix}$$

$$C_T = \begin{bmatrix} 0 & 0 & 0 & 1 \end{bmatrix},\ E_T = \begin{bmatrix} 0 & 0 \\ 0 & 0 \\ 0 & 0 \\ 0 & 0 \end{bmatrix}$$

On substituting value of A_T, B_T and U in equation (3.34), we get

$$X = \begin{bmatrix} I_{Lif} \\ V_L \\ V_{ci} \\ V_{cbi} \end{bmatrix} = \begin{bmatrix} -30.99 \\ 134.293 \\ 39.499 \\ 90.2258 \end{bmatrix} \tag{3.35}$$

The above equation (3.35) gives the steady state value of parameters and by knowing these values we can obtain the control to output voltage transfer function which can be further useful for controller design.

CHAPTER 4

MODELLING AND CONTROLLER DESIGN OF DUAL INPUT THREE PORT CONVERTER

4.1 INTRODUCTION

This chapter deals with control design of dual input three port converter. As we have discussed earlier about DI mode in chapter 2 and 3 in detail, we came to know from states 1-4 that output voltage is tightly regulated by S_1 having duty cycle D_1 whereas input voltage is regulated by S_3 having duty cycle D_3 i.e. power from the PV source is regulated at MPPT by IVR. In DI mode by battery is working in discharging mode.

The final control of the TPC working in DI mode can be done by using:

- MPPT Control- input voltage is controlled by MPPT.
- Output Voltage Control- output voltage is tightly regulated by S_1, having duty cycle D_1.

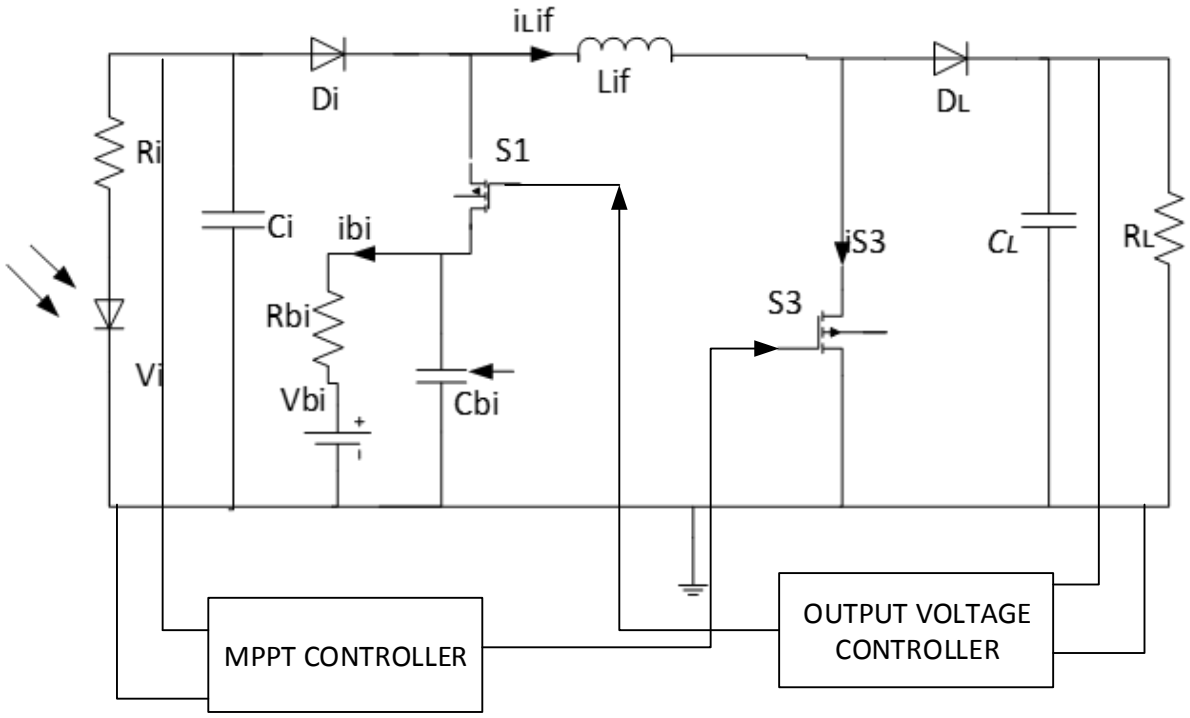

Fig. 4.1 Equivalent circuit of Boost-TPC in DI mode with MPPT control and output voltage control

4.2 MAXIMUM POWER POINT TRACKING (MPPT)

For PV to be future energy alternative source, it is essential to extract maximum power from panel but this is not so easy as its looking because the performance pf PV panel is affected by various conditions such as ambient temperature and irradiation. Thus, MPPT is used for such applications. MPPT compares the battery and PV output voltage, then it decides the best available power and voltage that the panel produces for charging the battery and to get maximum current in to the battery. It is effective during winters, hazy day and also when battery is discharged. The simplest algorithm is constant voltage algorithm in which load is set to $0.76V_{OC}$ of the PV panel. The drawback of this algorithm is that for measuring voltage panel is to be disconnected and thus power is lost so output get reduced.

4.2.1 PERTURB AND OBSERVE ALGORITHM

Mostly used algorithm is Perturb & Observe (P&O) due to its simplicity and reliability. In P&O algorithm. In this algorithm, array voltage is continuously perturbed i.e. incremented and decremented. The output power of the PV is periodically compared with previous perturbed cycle. If the power is positive, then direction of perturbation should be same, else direction of perturbation should reversed. Firstly, initialize the value of voltage and current, then read the power and voltage at kth instant. At next instant, again measure power and voltage at (k+1)th instant. Then subtract the voltage and power at (k+1)th instant and kth instant which is also known as change of voltage and power. If the change of power is positive, then check whether change in voltage is positive or negative. If change in voltage is positive then direction of perturbation is same but if change in voltage is negative then direction of perturbation is reversed. If the change of power is negative, then check whether change in voltage is positive or negative. If change in voltage is positive then direction of perturbation is reversed but if change in voltage is negative then direction of perturbation is same.

Table 4.1 Perturb & Observe Algorithm

Result	**Action**	**Command**
$\Delta P > 0$	$\Delta V > 0$	Increase voltage
$\Delta P > 0$	$\Delta V < 0$	Decrease voltage
$\Delta P < 0$	$\Delta V > 0$	Decrease voltage
$\Delta P < 0$	$\Delta V < 0$	Increase voltage

The flowchart for the perturb and observe (P&O) algorithm is shown below:

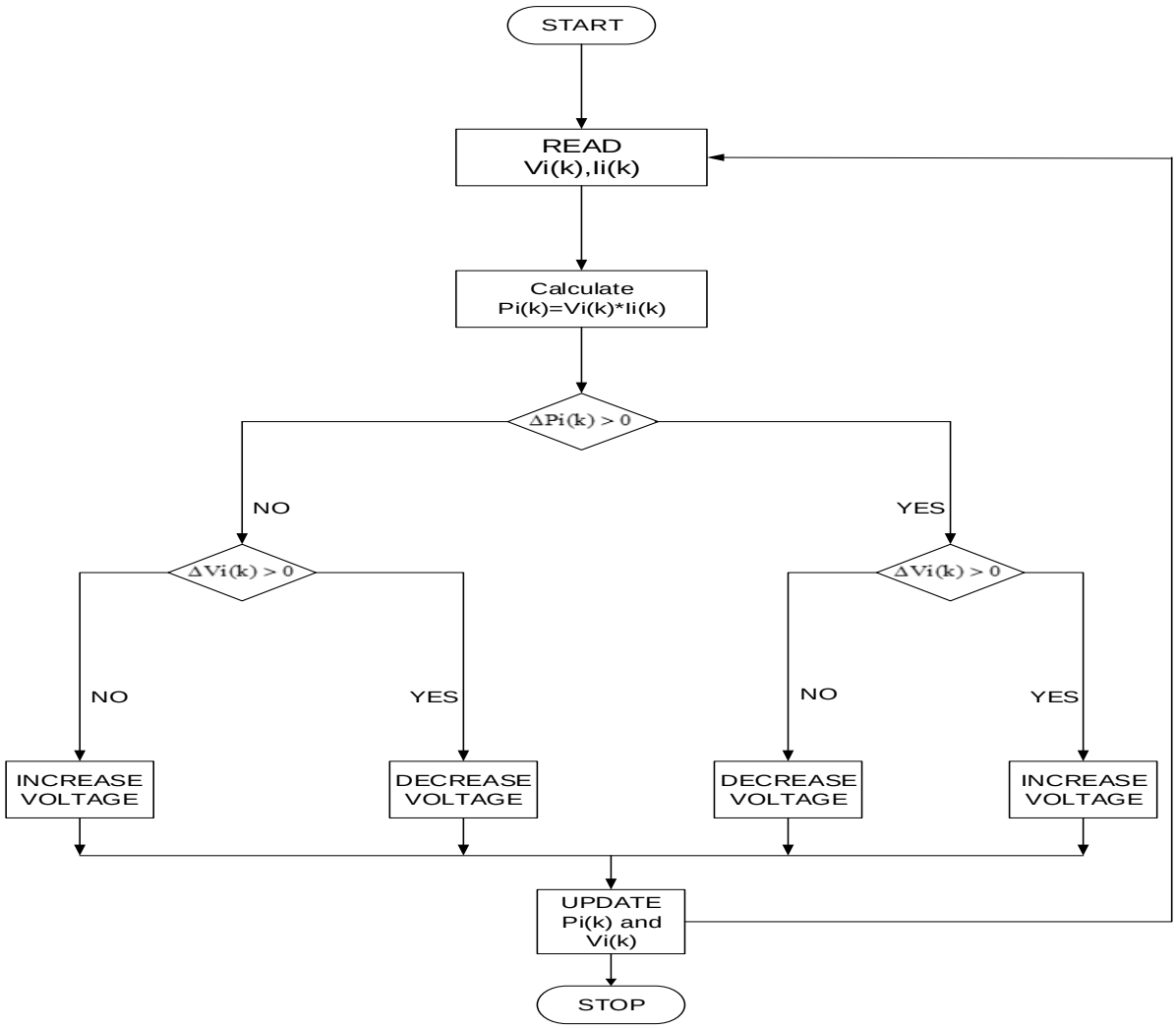

Fig. 4.2 Flowchart for the perturb and observe (P&O) algorithm

4.3 CONVERTER PARAMETER DESIGN

4.3.1 INDUCTOR DESIGN

The selection of appropriate inductor is very important in power converters and thus it's designing plays a major role in converter operation. In every power converters, inductance designing is so crucial because it is the heaviest part in converter. So small size and light weight inductance is very preferable in converters. The minimum value of inductance value which is required for the converter to operate in continuous conduction mode (CCM) is called as critical inductance. For the TPC the value of critical inductance depends on steady state value of input and output voltage, duty cycle, switching frequency and the output resistance.

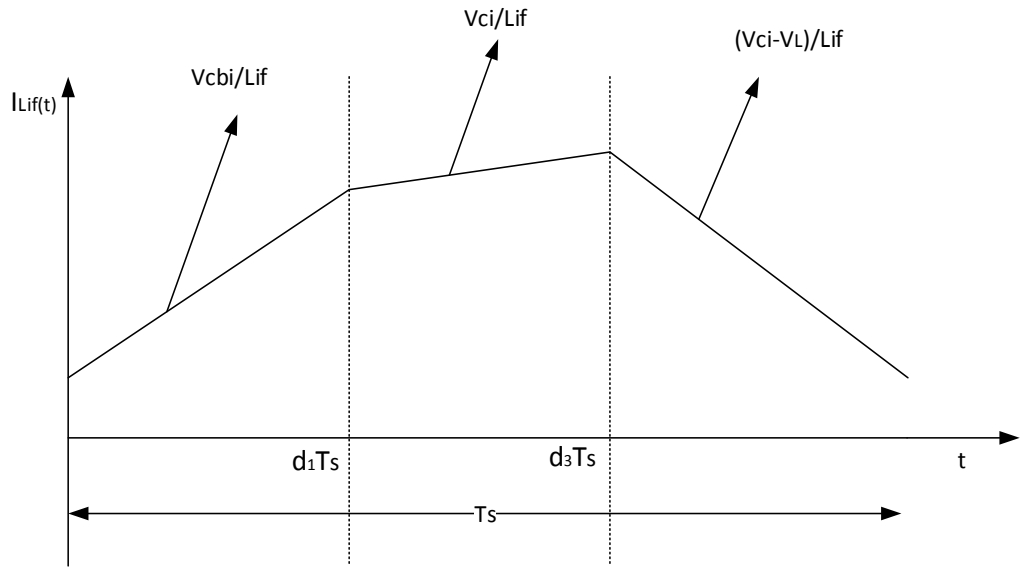

Fig. 4.3 Inductor current waveform

Thus, the value ripple current can be shown as:

$$2\Delta i_L = \frac{(\mathrm{V}_{ci} - \mathrm{V}_L)}{L_{if}}(1 - D_3)\,\mathrm{T}_S \tag{4.1}$$

The inductance of the TPC in DI mode is shown by below relation:

$$L_{if} = \frac{(\mathrm{V}_{ci} - \mathrm{V}_L)}{2\Delta i_L}(1 - D_3)\,\mathrm{T}_S \tag{4.2}$$

The value of ripple current can be so chosen such that it should be 10-20% of the load current. Thus, the inductance can be chosen such that ripple current should be minimum. For the designing of capacitors the following equations are shown below:

$$C_L = \frac{\left(\mathrm{I}_{Lif} + \frac{V_L}{R_L}\right)(1 - D_3)\,\mathrm{T}_s}{2\Delta v_L} \tag{4.3}$$

$$C_i = \frac{\left(\mathrm{I}_{Lif} + \frac{V_i - V_{ci}}{R_i}\right)(1 - D_1)\,\mathrm{T}_s}{2\Delta v_i} \tag{4.4}$$

$$C_{bi} = \frac{\left(\mathrm{I}_{Lif} + \frac{V_{cbi} - V_{bi}}{R_{bi}} \right) D_1 \mathrm{T}_s}{2\Delta v_{cbi}} \tag{4.5}$$

4.3.2 CONVERTER DESIGN SPECIFICATIONS

The parameters of the TPC has following specifications:

Table 4.2 Design Specification of Converter

PARAMETER	NOTATION	VALUES
PV panel voltage	V_i	40V
Battery voltage	V_{bi}	90V
Load voltage	V_L	135V
Switching frequency	f_s	100KHZ
Input capacitance	C_i	210uF
Load capacitance	C_L	680uF
Battery capacitance	C_{bi}	680uF
Inductance	L_{if}	65uH

CHAPTER 5

SIMULATION RESULTS AND CONCLUSION

5.1 SIMULATION RESULT

5.1.1 PV PANEL VOLTAGE

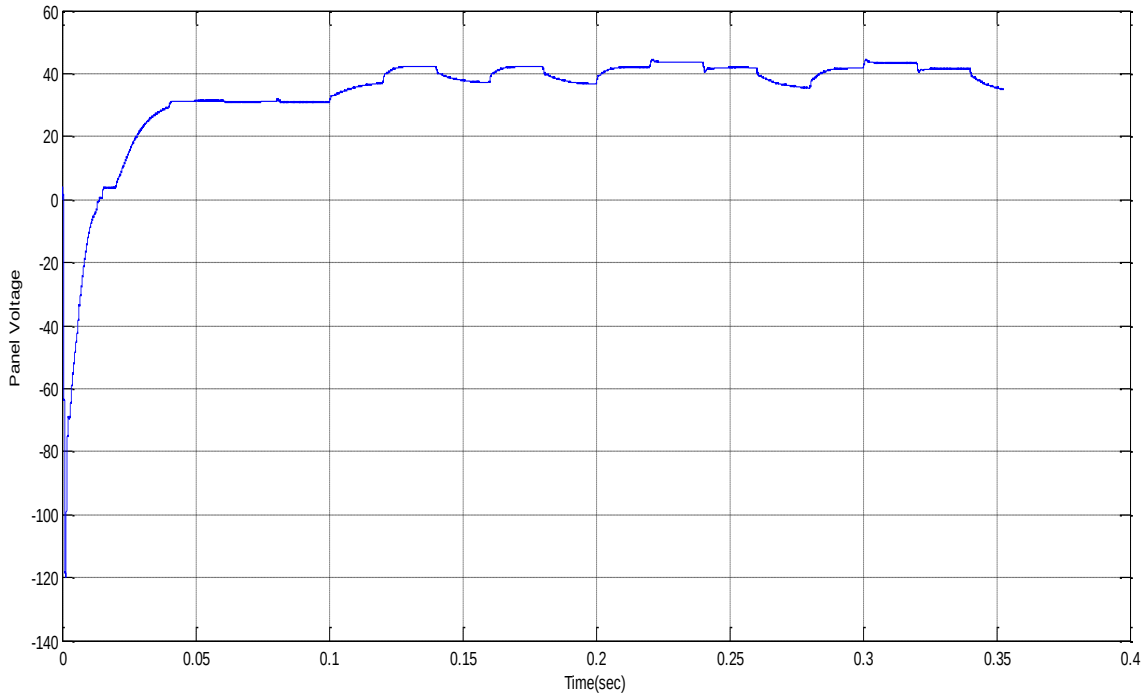

Fig. 5.1 Panel Voltage Vs Time Plot

5.1.2 PV PANEL CURRENT

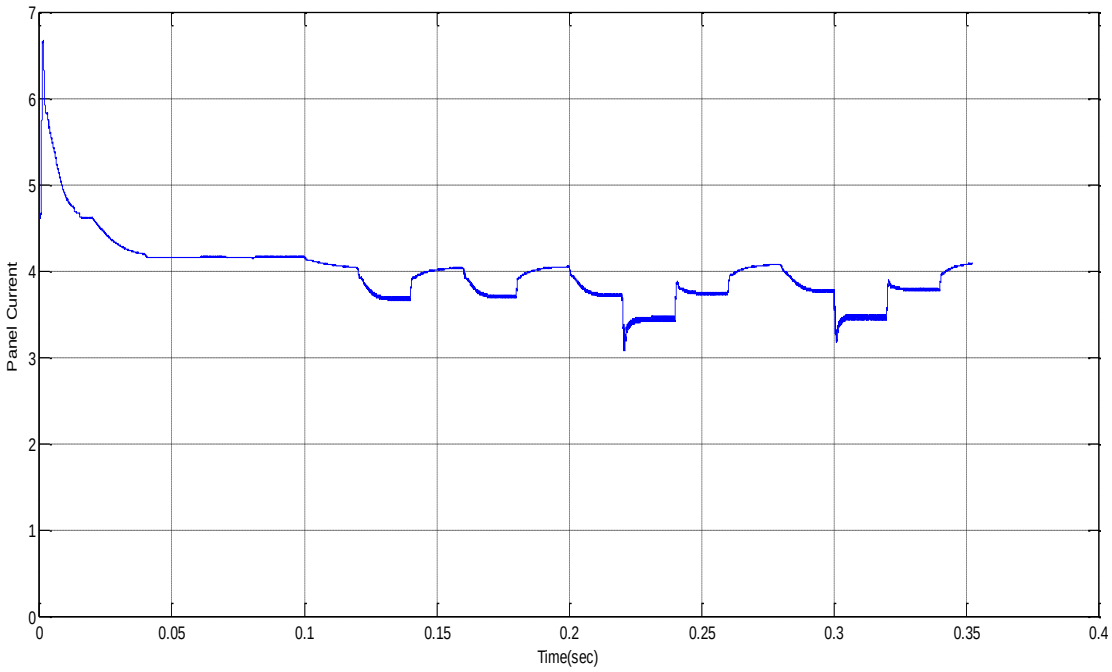

Fig. 5.2 Panel Current Vs Time Plot

5.1.3 DUTY CYCLE

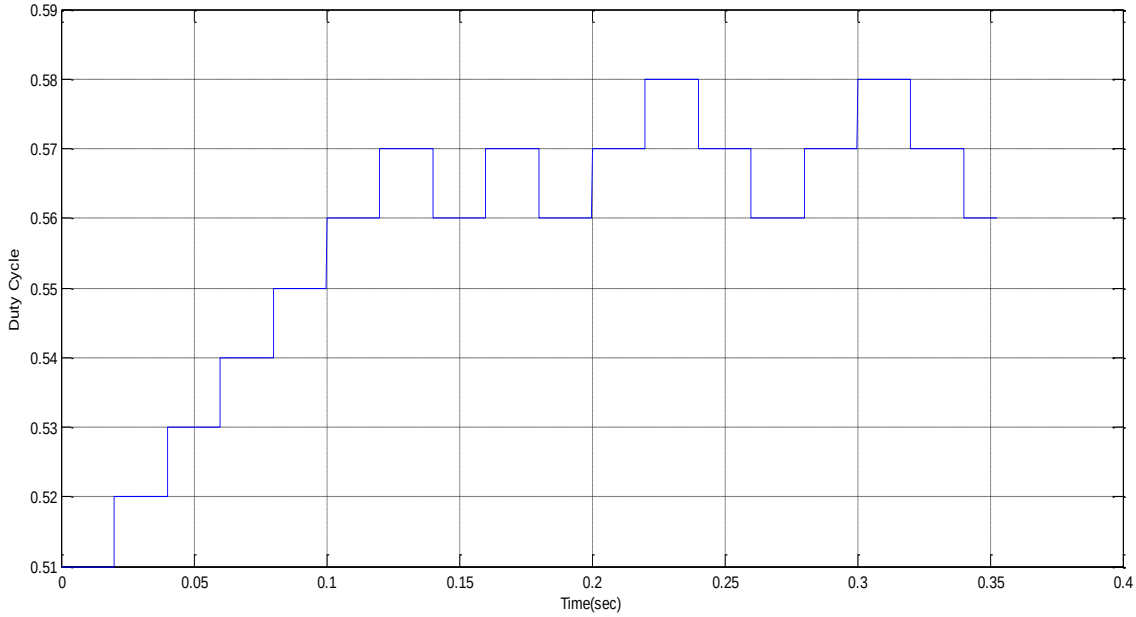

Fig. 5.3 Duty Cycle Vs Time Plot

5.1.4 OUTPUT VOLTAGE

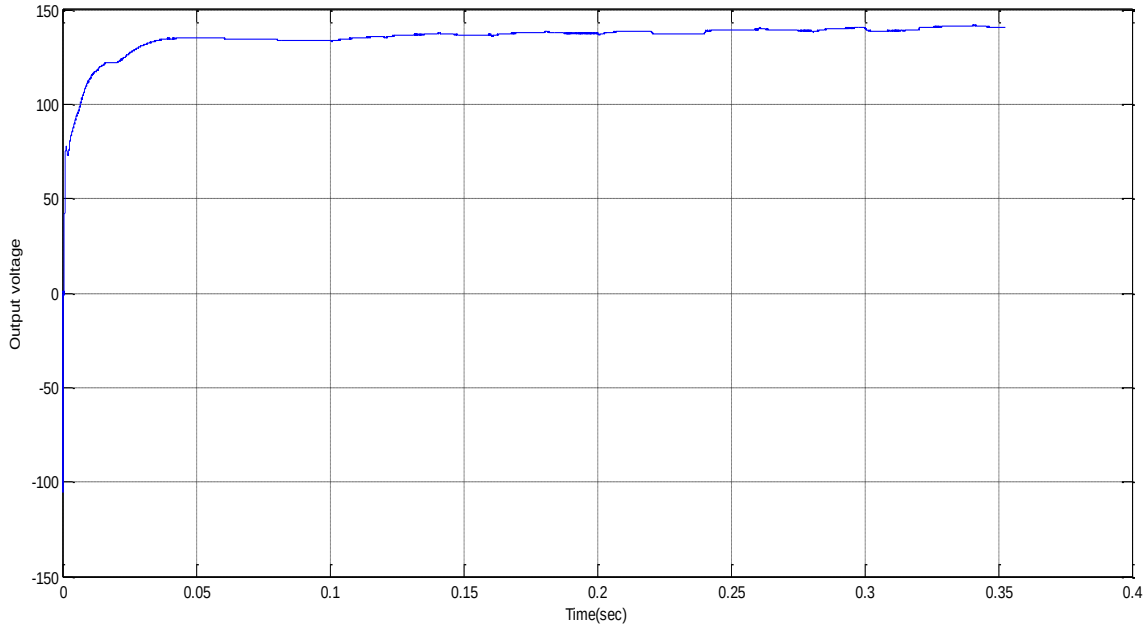

Fig. 5.4 Output Voltage Vs Time Plot

5.1.5 BATTERY CURRENT

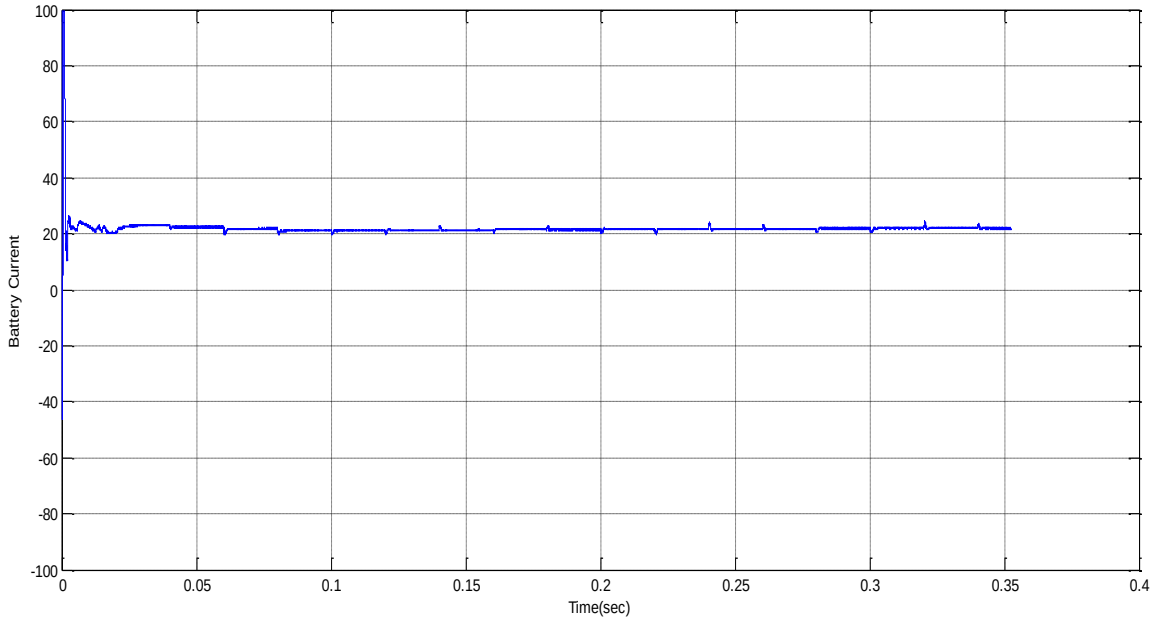

Fig. 5.5 Battery Current Vs Time Plot

Chapter 6

CONCLUSION

The three port converter (TPC) topology based on dual input converter (DIC) or dual output converter (DOC) interfaces one PV panel as input source port, one synchronous battery port, and an output/load port has been studied and analyzed. The steady state analysis, small signal modelling and state space averaging has been done for Boost-TPC in DI mode. The simulation result has verified the steady state analysis. The input panel voltage regulation is done by MPPT. The above simulation result shows that input PV panel voltage is tracking maximum power and reaching steady state whereas duty cycle, output load voltage are also reaching steady state. In DI mode as both battery and source is giving power to load, so we can say that battery will be functioning in discharging mode. Thus, from the result also it is verified that battery is discharging.

FUTURE WORK

This study provides another way to analyze power conversion in different TPC. Power management for multiple sources by using this analysis can also be studied in future. TPC can be working in three different modes so similar analysis can be done for both DO and SISO mode. An algorithm can also be developed in future in which TPC can be working in all three modes simultaneously depending on load requirement automatically.

.

BIBLOGRAPHY

[1]. Hongfei Wu,Kai Sun, Shun Ding, and Yan Xing, "Topology Derivation of Nonisolated Three-Port DC–DC Converters From DIC and DOC",*IEEE Trans. Power Electronics*, VOL. 28, NO. 7, pp. 3297-3307, JULY 2013.

[2]. Z. Qian, O. Abdel-Rahman, H. Al-Atrash, and I. Batarseh, "Modeling and control of three-port dc/dc converter interface for satellite applications", *IEEE Trans. Power Electron.*, vol. 25, no. 3, pp. 637–647, Mar. 2010.

[3]. S. Falcones and R. Ayyanar, "Simple control design for a three-port dc-dc converter based PV system with energy storage," presented at the *IEEE Appl. Power Electron. Conf, Palm Springs*, CA, 2010.

[4]. Y. Li, X. Ruan, D. Yang, F. Liu, and C. K. Tse, "Synthesis of multiple input dc/dc converters," *IEEE Trans. Power Electron.*, vol. 25, no. 9, pp. 2372–2385, Sep. 2010.

[5]. Y.-C. Liu and Y.-M. Chen, "A systematic approach to synthesizing multi input dc–dc converters," *IEEE Trans. Power Electron.*, vol. 24, no. 1,pp. 116–127, Jan. 2009.

[6]. Marcelo Gradella Villalva, Jonas Rafael Gazoli, and Ernesto Ruppert Filho, "Comprehensive Approach to Modeling and Simulation of Photovoltaic Arrays" , *IEEE Trans. Power Electron.*, vol. 24, no. 5, pp. 1198-1208, May. 2009.

[7]. M. A. Vitorino, L. V. Hartmann, A. M. N. Lima, and M. B. R. Correa, "Using the model of the solar cell for determining the maximum power point of photovoltaic systems," in *Proc. Eur. Conf. Power Electron*. Appl., 2007, pp. 1–10.

[8]. W. Jiang and B. Fahimi, "Multiport power electronic interface—Concept, modeling and design," *IEEE Trans. Power Electron.*, vol. 26, no. 7, pp. 1890–1900, Jul. 2011.

[9]. K Haribaran and NedMohan, "Three-port series-resonant dc–dc converter to interface renewable energy sources with bidirectional load and energy storage ports," *IEEE Trans. Power Electron.*, vol. 24, no. 10, pp. 2289–2297, Oct. 2009.

[10]. H. Wu, K. Sun, R. Chen, H. Hu, and Y. Xing, "Full-bridge three-port converters with wide input voltage range for renewable power systems," *IEEE Trans. Power Electron.*, vol. 27, no. 9, pp. 3965–3974, Sep. 2012.

[11]. F. Nejabatkhah, S. Danyali, S. H. Hosseini, M. Sabahi, and S. M. Niapour, "Modeling and control of a new three-input dc-dc boost converter for hybrid PV/FC/battery power system," *IEEE Trans. Power Electron.,* vol. 27, no. 5, pp. 2309–2324, May 2012.

[12]. C. N. Onwuchekwa and A. Kwasinski, "A modified-time-sharing switching technique for multiple-input dc–dc converters*," IEEE Trans. Power Electron.,* vol. 27, no. 11, pp. 4492–4502, Nov. 2012.

[13]. N. Femia, G. Petrone, G. Spagnuolo, "Optimization of Perturb and Observer Maximum Power Point Tracking Method" *IEEE Transactions on Power Electronics,* VOL. 20, NO. 4. July 2005.

[14]. Yu-Lung Ke, Ying-Chun Chuang, Yuan-Kang Wu and Bo-Tsung Jou, "Implementation of a Solar Power Battery Energy Storage System with Maximum Power Point Tracking," *IEEE Ind. Applications Society Annu. Meeting (IAS),* pp.1-8, Oct. 2010.

[15]. E. Koutroulis and K. Kalaitzakis, "Novel battery charging regulation system for photovoltaic applications," *IEE Proceedings - Electric Power Applications,* vol.151, no.2, pp. 191- 197, Mar 2004.

[16]. J. L. Duarte, M. A. M. Hendrix, and M. G. Simoes, "Three-port bidirectional converter for hybrid fuel cell systems*," IEEE Trans. Power Electron*., vol. 22, no. 2, pp. 480–487, Mar. 2007.

[17]. H. Tao, J. L. Duarte, and M. A. M. Hendrix, "Multiport converters for hybrid power sources," in Proc. *IEEE Power Electron. Spec. Conf.* , 2008, pp. 3412–3418.

[18]. S. Malo and R. Grino, "Design, construction, and control of a stand-alone energy-conditioning system for PEM-type fuel cells," *IEEE Trans. Power Electron.,* vol. 25, no. 10, pp. 2496–2506, Oct. 2010.

[19]. K. Sun, L. Zhang,Y. Xing, and J. M.Guerrero, "Adistributed control strategy based on dc bus signaling for modular photovoltaic generation systems with battery energy storage," *IEEE Trans. Power Electron.,* vol. 26, no. 10, pp. 3032–3045, Oct. 2011.

[20]. S. Malo and R. Grino, "Design, construction, and control of a stand-alone energy-conditioning system for PEM-type fuel cells," *IEEE Trans. Power Electron.,* vol. 25, no. 10, pp. 2496–2506, Oct. 2010.